ADVANCED MATERIALS

separation of the three phases to form the coaxial nanostructure. Our composite nanocable structure with a crystalline silicon core should be an interesting candidate for nanoelectronic devices. Meanwhile, the present method can be further explored to engineer other multilayer nanojunctions with the desired geometry.

Received: June 19, 2000
Final version: August 16, 2000

[1] R. Tenne, M. Homyonfer, Y. Feldman, *Chem. Mater.* **1998**, *10*, 3225.
[2] X. Blase, J.-C. Charlier, A. De Vita, R. Car, *Appl. Phys. A* **1999**, *68*, 293.
[3] Y. Zhang, K. Suenaga, C. Colliex, S. Iijima, *Science* **1998**, *281*, 973.
[4] Y. Zhang, H. Gu, K. Suenaga, S. Iijima, *Chem. Phys. Lett.* **1997**, *179*, 264.
[5] K. Suenaga, C. Colliex, N. Demoncy, A. Loiseau, H. Pascard, F. Willaime, *Science* **1997**, *278*, 652.
[6] K. Suenaga, M. P. Johansson, N. Hellgren, E. Broitman, L. R. Wallenberg, C. Colliex, J.-E. Sundgren, L. Hultman, *Chem. Phys. Lett.* **1999**, *300*, 695.
[7] K. Suenaga, F. Willaime, A. Loiseau, C. Colliex, *Appl. Phys. A* **1999**, *68*, 301.
[8] W. Han, Y. Bando, K. Kurashima, T. Sato, *Chem. Phys. Lett.* **1999**, *299*, 368.
[9] E. W. Wong, B. W. Maynor, L. D. Burns, C. M. Lieber, *Chem. Mater.* **1996**, *8*, 2041.
[10] W. Han, S. Fan, Q. Li, Y. Hu, *Science* **1997**, *277*, 1287.
[11] W. Han, S. Fan, Q. Li, W. Liang, B. Gu, D. Yu, *Chem. Phys. Lett.* **1997**, *265*, 374.
[12] W. Han, P. Redich, F. Emst, M. Ruhle, *Appl. Phys. Lett.* **1999**, *75*, 1875.
[13] E. I. Givargizov, *J. Cryst. Growth* **1975**, *31*, 20.
[14] J. Westwater, D. P. Gosain, S. Usui, *Phys. Status Solidi A* **1998**, *165*, 37.
[15] A. M. Morales, C. M. Lieber, *Science* **1998**, *279*, 208.
[16] W. S. Shi, H. Y. Peng, N. Wang, S. T. Lee, *J. Am. Ceram. Soc.*, in press.
[17] F. Danes, E. Saint-Aman, L. Coudurier, *J. Mater. Sci.* **1993**, *28*, 489.
[18] N. Wang, Y. H. Tang, Y. F. Zhang, C. S. Lee, I. Bello, S. T. Lee, *Chem. Phys. Lett.* **1999**, *299*, 237.
[19] H. Hofmeister, J. Dutta, H. Hofmann, *Phys. Rev. B* **1996**, *54*, 2856.
[20] H. Hofmeister, P. Kodderitzsch, U. Gösele, *Ber. Bunsenges. Phys. Chem.* **1997**, *101*, 1647.

Assembly of Micropatterned Colloidal Gold Thin Films via Microtransfer Molding and Electrophoretic Deposition**

By *Ryan C. Bailey*, *Keith J. Stevenson*, and *Joseph T. Hupp**

The ability to fabricate materials and structures with submicrometer scale features reliably and economically is of interest in many areas of science and technology. For instance, significant and vigorous research efforts are focused on controlling the assembly of inorganic and metallic nanoscopic particles.[1–5] This interest has arisen because these nanostructured materials often exhibit properties that are remarkably different from those of materials of macroscopic dimensions, for example, quantum-confined size-tunable luminescence behavior,[6] Coulomb staircase effects,[7] and photonic band-gap responses.[8] Metallic gold colloids, in particular, have been intensely investigated with the intent to elucidate fundamental behavior and to find materials with interesting new properties.[9–12] One specific goal is to tailor the size, shape, and geometrical arrangement of nanoscopic particles, clusters, and aggregates in an effort to produce desired linear and nonlinear optical properties such as specifically tuned spectral extinction[13,14] or optimization of localized electromagnetic surface enhancement phenomena.[15,16]

To date the majority of the methods used to assemble colloidal gold thin films have been based on adsorption from colloidal solutions onto chemically derivatized surfaces with a specific affinity for Au, for example, amines ($-NH_2$), thiols (–SH), and carboxylic acids (–COOH).[17–22] While they are very effective for preparation of densely packed nanoparticle thin films, these methods have certain drawbacks in that: 1) the time scale for assembly is generally slow (hours to days), 2) surface particle density is sometimes difficult to regulate, and 3) in the simplest cases, no significant patterning of the particles occurs. These drawbacks are largely a consequence of dealing with colloidal solutions containing very small particles (<300 nm diameter). In this size regime, colloidal forces, i.e., buoyancy, frictional, and coulombic forces, outweigh the gravitational (sedimentation) force and act to keep the particles suspended. Consequently, particle transport is governed solely by Brownian motion, resulting in completely random particle–particle and particle–substrate collisions.

In an attempt to circumvent some of these limitations, recent studies have focused on creating templated nanoparticle assemblies using methods such as microcontact printing of self-assembled monolayers (SAMs),[23,24] nanoetching,[25] and e-beam lithography[26] to fabricate spatially and density controlled nanoparticle architectures. We are also interested in developing low-cost approaches to fabricating nanoparticle assemblies—in particular, assemblies capable of functioning as 2D optical transmission gratings for chemical sensing applications. Herein we describe a straightforward method for the assembly of micropatterned colloidal gold thin films on conducting platforms that relies upon electrophoretic deposition and a form of soft lithography, microtransfer molding (μTM).[27,28]

Since colloidal metal particles are usually charged, a promising approach is to utilize a directional force (an external electric field) to drive the suspended nanoscopic particles toward a surface. This process, known as electrophoretic deposition (EPD), permits external regulation of surface nanoparticle density and film growth. Surprisingly, despite the extensive use of EPD in materials synthesis,[29–32] in only a few cases has it been employed for the assembly of thin films of metal nanoparticles.[33–36] Most relevant to our report, are reports by Giersig and Mulvaney on the electrophoretic deposition of gold colloids from aqueous and organic media onto transmission electron microscopy (TEM) grids.[35,36] Here we report an elaboration of the electrophoresis

[*] Prof. J. T. Hupp, R. C. Bailey, Dr. K. J. Stevenson
Department of Chemistry and
Center for Nanofabrication and Molecular Self-Assembly
Northwestern University
Evanston, IL 60208 (USA)
E-mail: jthupp@chem.nwu.edu

[**] We thank the Office of Naval Research for financial support, and Professor R. P. Van Duyne, Ms. Christy Haynes, Ms. Michelle Duval, and Mr. Adam McFarland for assistance with spatially resolved UV-vis extinction measurements.

  0935-9648/00/2412-1930 $ 17.50+.50/0

approach that yields patterned, rather than monolithic, thin films of colloidal gold.

In order to perform electrophoretic deposition, an applied directional force that drives the colloid towards the substrate must overcome the natural forces of gravitation, buoyancy, and friction. When the magnitude of the force that a colloid experiences in the presence of an electric field ($F_E = Q_E E$) is greater than the natural forces on the particles ($F_N = \nu 3\pi\eta d$)[37] then the particles can be manipulated by the field. Using the reported zeta potential ($\zeta = -35$ mV) of a citrate-stabilized 14 nm colloidal gold particle in aqueous solution, its velocity can be calculated to determine the magnitudes of forces acting on the particle. When a voltage of +0.250 V is applied then $F_E > F_N$. At this potential (or correspondingly when the electric field exceeds ~1.25 V/cm) we expect to observe controlled assembly via electrophoretic deposition; at potentials below this threshold value no substantial field-assisted colloidal deposition is expected.

Figure 1 summarizes the fabrication strategy: A polydimethylsiloxane (PDMS) stamp created from a lithographic master was used to pattern an organic soluble ink (Shipley photoresist 1827) on indium tin oxide (ITO) using a previously described procedure,[27] commonly referred to as μTM.[28] The colloidal Au negative pattern was then generated via electrophoretic deposition by applying an anodic bias of +0.250 V to the ITO platform for 60 min in the presence of a 1 mM citrate-stabilized Au colloid solution. Subsequent soaking of the patterned substrate in acetone for 15 min removed the soluble organic ink template. Film deposition is observed to occur at precisely the predicted applied potential. The field required for patterned assembly (less than 1.3 V/cm) is surprisingly small in comparison to fields typically used in EPD of ceramic films (~50–200 V/cm),[38] but in agreement with earlier findings.[35] No colloids are observed to deposit in the absence of an electric field, nor under conditions of cathodic bias, even over long periods of time (>5 h). Although the mechanism for film growth is not fully understood, adsorption of the negatively charged particles at the positively charged electrode obviously is strong enough to overcome repulsive particle–particle electrostatic interactions. Recent investigations of field-induced colloidal film assembly indicate that both electroosmotic[39] and electrohydrodynamic[40] transport processes can act to drive fluid and particle motion.

Figure 2 shows representative atomic force microscopy (AFM) images of a patterned colloidal gold film prepared from PDMS stamps made from a lithographic master with 5 μm × 5 μm square relief structures. Good replication is observed (Fig. 2a), with a pattern that is remarkably uniform over areas greater than 5 mm^2, as governed by the nominal size of the PDMS stamp employed. A clearer view of the nanoscale structure and component particle composition is shown in Figure 2b. The templated regions appear to be composed of discrete, densely packed particles, with a higher degree of clustering occurring at the patterned boundaries (edges). Figure 2c is a higher resolution image of the region indicated in Figure 2b that shows individual colloids as well as two- and three-dimensional aggregates. Although accurate size and spacing information cannot be directly obtained from unprocessed AFM images due to convolution of the particle with the tip (which leads to a broadening of the lateral dimensions), analysis of particle height should give a good indication of the particle (sphere) size.[41] Surprisingly, the patterned areas appear to be only a monolayer thick, as demonstrated by the histogram plot (Fig. 2d) obtained by performing "bear-

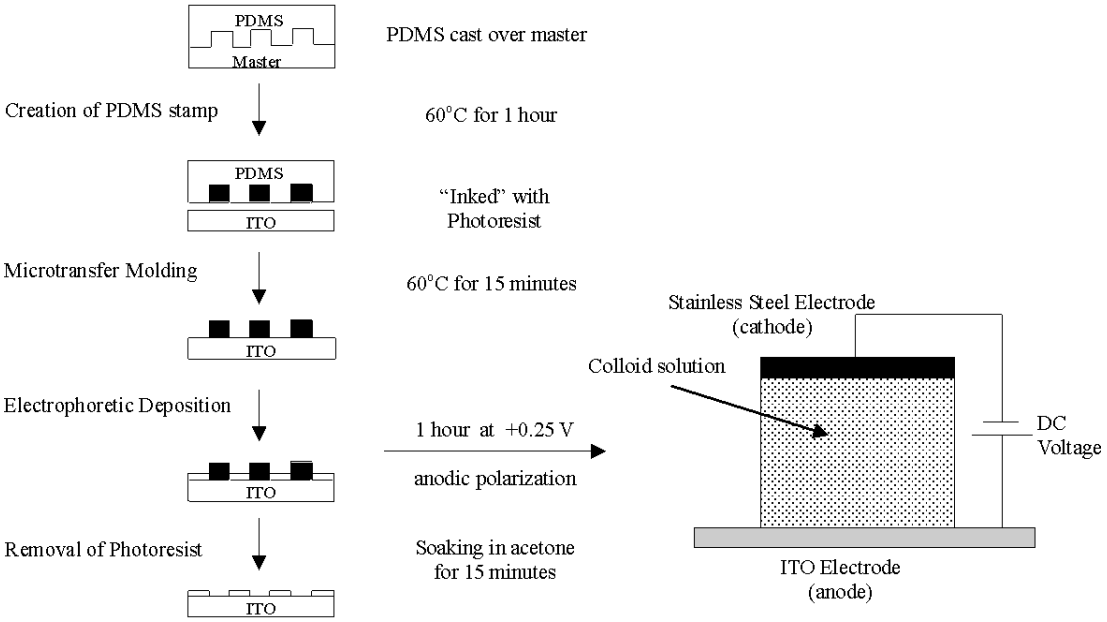

Fig. 1. Procedure for fabrication of patterned colloidal gold thin films on transparent, conductive ITO substrates via microtransfer molding and electrophoretic deposition. Left: Formation of a PDMS stamp and patterned ITO substrate. Right: Schematic representation of the electrophoretic deposition cell consisting of a stainless steel cathode and an ITO anode. Adjustment of the applied electric field gradient is accomplished by variation of the DC voltage and cathode–anode gap spacing.

  0935-9648/00/2412-1931 $ 17.50+.50/0

ADVANCED MATERIALS

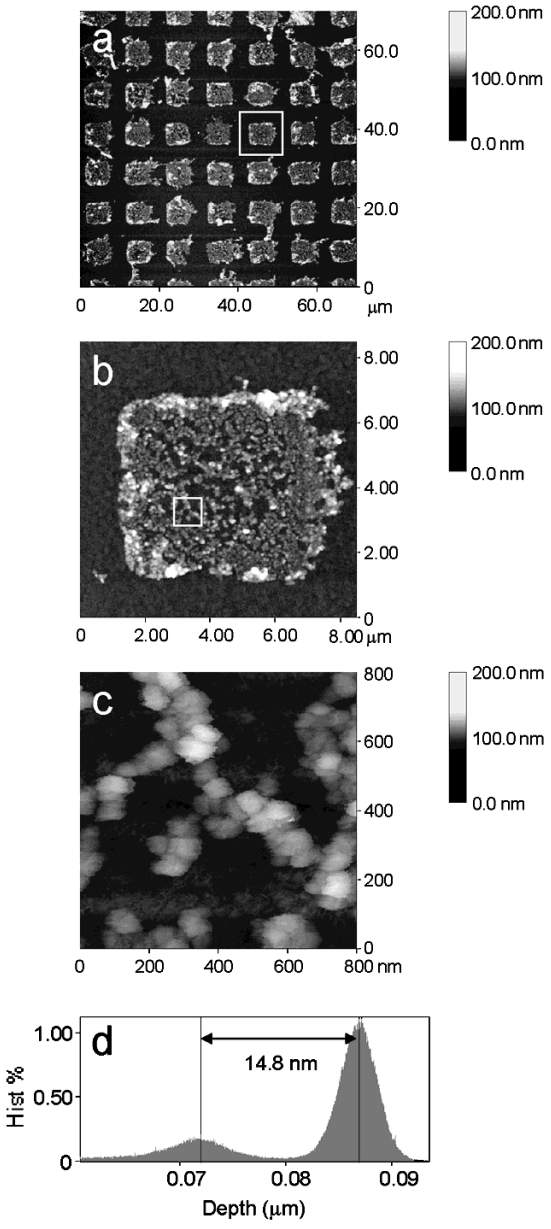

Fig. 2. a) Representative 70 μm × 70 μm AFM height image of a micropatterned gold colloid thin film prepared by μTM and electrophoretic deposition. b) 8.25 μm × 8.25 μm AFM height image of the area indicated by the white box in (a). c) A higher resolution 0.8 μm × 0.8 μm AFM height image of the area outlined by the white box in (b), showing individual and aggregated colloids. d) Depth histogram obtained by "bearing" analysis of (b) showing that resultant patterned colloidal films are roughly one monolayer thick (particle height 15 nm).

ing analysis".[42] The average patterned film thickness is estimated to be 15 nm, consistent with the colloidal solution particle size (14 nm). Using a 2D space-filling argument and assuming that a full closest packed monolayer will occupy 74.05 % of the area inside the squares, we have estimated the surface particle concentration to be ~2.4×10^{11} particles/cm^2, a density slightly higher (approximately 30 % greater) than that observed by self-assembly methods.[17-22]

Scanning electron microscopy (SEM) and energy dispersive X-ray spectroscopy (EDX) were also used to characterize film nano- and microstructure. Consistent with the AFM data and with light microscopy, extended micropatterning was also observed (data not shown). EDX was used to verify the presence of gold (peak at 2.150 keV), as shown in Figure 3. The EDX spectrum in Figure 3a, obtained on a single patterned square, also shows the presence of silicon (1.735 keV), indium (3.310 keV), and tin (3.460 keV). The EDX spectrum in Figure 3b was acquired from a bare section between the patterned area and shows only peaks for Si, In, and Sn.

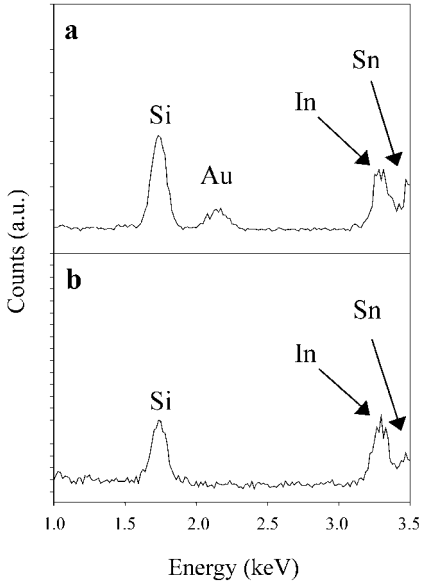

Fig. 3. EDX point spectra acquired from a) a Au colloid square region of a patterned film and b) a bare ITO region between the squares.

The optical properties of the patterned films were examined by UV-vis extinction spectroscopy. Figure 4 shows spectra for a 33 μM aqueous colloidal solution of 14 nm gold particles (Fig. 4, dotted line) and a micropatterned film (Fig. 4, solid

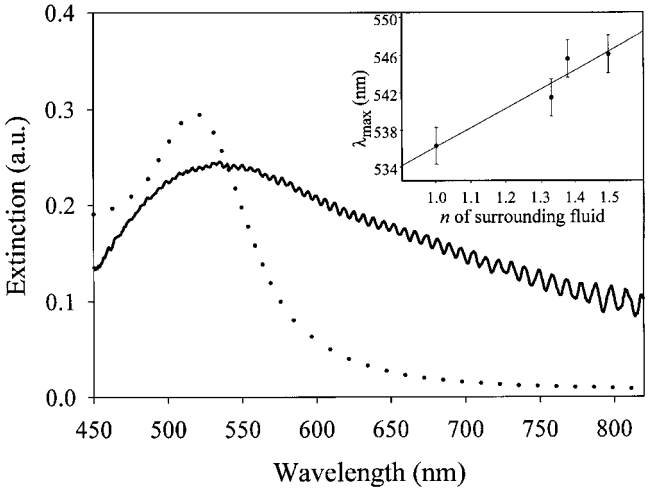

Fig. 4. Extinction spectra of a 33 μM aqueous colloidal Au solution (dotted line, λ_{max} = 524 nm) and a micropatterned colloidal Au thin film (solid line, λ_{max} = 536 nm) demonstrating the red-shift associated with interacting particles and aggregates. Inset: Plot comparing the maximum extinction wavelength (λ_{max}) under different refractive index fluids and showing the red-shift associated with increasing the dielectric environment of the colloidal particles.

  0935-9648/00/2412-1932 $ 17.50+.50/0

line). The extinction maximum of the former appears at 524 nm, as expected,[43] but in the latter occurs at 536 nm. We attribute the 12 nm shift for the film to the high refractive index environment imposed on one side of the film by the ITO platform.[44] The high-index environment is also expected to broaden and dampen the plasmon absorption.

Broadening is also expected based on many-particle interactions, as is a filling-in of the red portion of the spectrum.[13] The plasmon resonance can be additionally red-shifted by introducing a fluid with a higher refractive index than air. The inset in Figure 4 shows the shift in the extinction maximum as the surrounding medium is changed from air (n = 1.00, λ_{max} = 536 nm) to water (n = 1.332, λ_{max} = 541 nm) to hexane (n = 1.379, λ_{max} = 545 nm), and finally to benzene (n = 1.498, λ_{max} = 546 nm). This behavior is consistent with that observed for platform-supported gold colloid monolayers[45] as well as for gold colloid solutions.[46]

Lastly, we find that the patterned films are capable of functioning as transmissive 2D optical diffraction gratings. The requirements for diffraction are well-defined periodic compositional differences and significant differences in refractive index, n, for the compositionally distinct areas. Diffraction is expected to be most efficient when the diffraction elements have heights comparable to the wavelength of incident light (such that the electromagnetic radiation interacts with the grating elements over a full period). Nevertheless, even with a periodic film of ~15 nm thickness, transmissive diffraction of a He–Ne laser beam (λ = 632.8 nm) is readily observable by eye. The inset in Figure 5 shows a 2D pattern recorded with a microstructured colloidal gold film in air.

Since diffraction is a result of periodic modulation in the refractive index of a system (e.g., air–gold–air), it follows that as the index of the surrounding medium is increased, the relative amount of light diffracted will diminish. Knowing that the first-order diffraction efficiency of a system scales as the square of the difference of the refractive indices of the two components,[47] it is possible to gain information regarding the grating by monitoring the relative amount of diffracted light in varying dielectric environments. Figure 5 demonstrates this effect: The square root of the intensity of a first-order diffraction peak ($I_{1,0}$; see Fig. 5, inset) is plotted versus the refractive index of the surrounding fluid. As expected, the intensity decreases as n_{fluid} increases. Extrapolation of the plot to zero diffracted-light intensity should define the point where n_{fluid} matches the refractive index of the gold nanoparticle film. For λ = 633 nm, the value obtained (admittedly via lengthy extrapolation) is ~3.2. We note that the film refractive index should be wavelength dependent and for gold will contain both real and imaginary components. Strictly speaking, the refractive index of the gold film should itself also change slightly as n_{fluid} changes, since n_{fluid} can influence the plasmon absorption energy (see inset in Fig. 4). This, in turn, will change the degree of resonance enhancement of the index at a fixed diffraction wavelength. While the likely small influence of n_{fluid} upon the refractive index of the film has been ignored here, we note that essentially the same effect is responsible for the exquisite sensitivity of surface plasmon resonance spectroscopy to interfacial adsorption.[48] We suggest that with an appropriate choice of incident-light color, a similar sensitivity to molecular or ionic absorption might be achievable based on changes in diffraction efficiency.

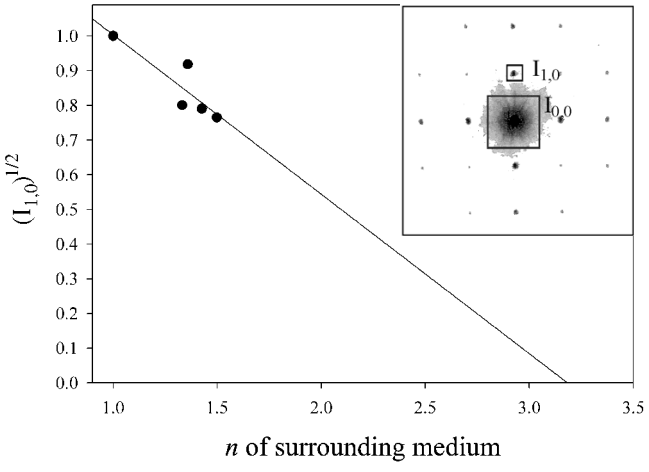

Fig. 5. Plot of square root of relative first-order ($I_{1,0}$) diffraction peak intensity versus external solvent refractive index (n). Inset: Two-dimensional optical diffraction pattern produced by transmission of light from a He–Ne laser (632.8 nm) through a micropatterned colloidal gold thin film.

In summary, we report a convenient approach to controlled fabrication of ultra-thin micropatterned colloidal gold films on conductive platforms using a combination of microtransfer molding and electrophoretic deposition techniques. When the platforms consist of transparent, ITO-coated glass, the films readily diffract visible light. We suggest that these and related micropatterned films may prove useful as chemo- and electrochemically responsive optical diffraction gratings.[49–54]

Experimental

Stamps and Platforms: Patterned PDMS stamps were prepared from Dow Corning Sylgard 184 (Ellsworth) cured for 1 h at 60 °C on a lithographic master (10 μm pitch AFM calibration grating, Digital Instruments) having a two-dimensional 5 μm × 5 μm square relief structure. Transparent, conductive ITO platforms (10 Ωsquare, Delta Technologies) were cleaned by immersion for 15 min in a heated (80 °C) aqueous solution of ethanolamine (Aldrich, 20 wt.-%), followed by rinsing several times with deionized water.

Patterning and Film Deposition: Patterning was accomplished by employing a soft lithography process known as μTM [28]. Wet inking of the patterning material involved placing a drop of a diluted solution (1:10 (v/v) ink/acetone) of commercially available photoresist (Shipley, 1827) on the PDMS stamp. The inked PDMS stamp was then quickly placed onto a clean ITO platform and a light weight (~10 g/cm^2) was applied to the top of the stamp to ensure uniform contact. The ITO–photoresist–PDMS mold was then cured at 60 °C for 5 min.

Subsequently, the patterned ITO substrate solution was introduced into the custom fabricated electrophoretic cell (see Fig. 1) containing an aqueous gold colloid solution (1.0 mM) prepared by a literature method [55].

A BAS CV27 (Bioanalytical Systems) potentiostat configured in a two-electrode arrangement was used for electrophoretic deposition. The cell allowed the distance between the anode and the cathode electrodes to be adjusted to an optimum distance of 2 mm. Optimal coverage was observed when deposition was carried out for 1 h, and the ITO was biased at +0.25 V (versus Pt counter electrode) for electrophoretic deposition. Following the deposition, the photoresist was removed by simply soaking the substrate in acetone for 15 min.

Surface Characterization: AFM measurements were obtained using a Digital Instruments Multimode Nanoscope IIIa operating in tapping mode using a single-etched silicon (TESP) Nanoprobe SPM tip (cantilever length 125 μm and

  0935-9648/00/2412-1933 $ 17.50+.50/0

ADVANCED MATERIALS

resonance frequency 307–367 Hz, Digital Instruments). Solution UV-vis spectra were obtained on a HP 8452A diode array spectrophotometer. Spatially resolved UV-vis microextinction measurements were performed using a previously published procedure [56]. EDX spectra were obtained on a Hitachi 4500 FE-SEM operating at 20 kV. A He–Ne laser (λ = 632.8 nm, 5 mW, Uniphase) was used for the diffraction measurements. A digital zoom camera (Kodak) was used to capture the diffraction pattern.

Received: June 7, 2000

[1] J. P. Novak, D. L. Feldheim, *J. Am. Chem. Soc.* **2000**, *122*, 3979.
[2] A. K. Boal, F. Ilhan, J. E. DeRouchey, T. Thurn-Albrecht, T. P. Russell, V. M. Rotello, *Nature* **2000**, *404*, 746.
[3] R. Maoz, E. Frydman, S. R. Cohen, J. Sagiv, *Adv. Mater.* **2000**, *12*, 424.
[4] N. Kimizuka, M. Tanaka, T. Kunitake, *Chem. Lett.* **1999**, *12*, 1333.
[5] J. H. Holtz, J. S. W. Holtz, C. H. Munro, S. A. Acher, *Anal. Chem.* **1998**, *70*, 780.
[6] A. P. Alivisatos, *Science* **1996**, *271*, 933.
[7] R. S. Ingram, M. J. Hostetler, R. W. Murray, T. G. Schaaff, J. T. Kohourt, R. L. Whetten, T. P. Bigioni, D. K. Guthrie, P. N. First, *J. Am. Chem. Soc.* **1997**, *119*, 9279.
[8] M. D. B. Charlton, G. J. Parker, *J. Micromech. Microeng.* **1998**, *8*, 172.
[9] A. Doron, E. Katz, I. Willner, *Langmuir* **1995**, *11*, 1313.
[10] P. Xu, H. Yanagi, *Chem. Mater.* **1999**, *11*, 2626.
[11] D. Meisel, W. A. Mulac, M. S. Matheson, *J. Phys. Chem.* **1981**, *85*, 179.
[12] K. E. Gonsalves, G. Carlson, J. Kumar, F. Aranda, M. Jose-Yacamon, *Nanotechnology* **1996**, *622*, 151.
[13] M. L. Sandrock, C. A. Foss, *J. Phys. Chem. B* **1999**, *103*, 11 398.
[14] L. A. Lyon, D. J. Pena, M. J. Natan, *J. Phys. Chem. B* **1999**, *103*, 5826.
[15] L. A. Lyon, M. D. Musick, M. J. Natan, *Anal. Chem.* **1998**, *70*, 5177.
[16] J. B. Broderick, M. J. Natan, T. V. O'Halloran, R. P. Van Duyne, *Biochemistry* **1993**, *32*, 13 771.
[17] K. C. Grabar, R. G. Freeman, M. B. Hommer, M. J. Natan, *Anal. Chem.* **1995**, *67*, 735.
[18] K. C. Grabar, P. C. Smith, M. D. Musick, J. A. Davis, D. G. Walter, M. A. Jackson, A. P. Guthrie, M. J. Natan, *J. Am. Chem. Soc.* **1996**, *118*, 1148.
[19] K. C. Grabar, K. J. Allison, B. E. Baker, R. M. Bright, K. R. Brown, R. G. Freeman, A. P. Fox, C. D. Keating, M. D. Musick, M. J. Natan, *Langmuir* **1996**, *12*, 2353.
[20] H. Fan, G. P. Lopez, *Langmuir* **1997**, *13*, 119.
[21] F. Tian, K. J. Klabunde, *New. J. Chem.* **1998**, *22*, 1275.
[22] J. Schmitt, P. Machtle, D. Eck, H. Mohwald, C. A. Helm, *Langmuir* **1999**, *15*, 3256.
[23] J. Zheng, Z. Zhu, H. Chen, Z. Liu, *Langmuir* **2000**, *16*, 4409.
[24] H. X. He, H. Zhang, Q. G. Li, T. Zhu, S. F. Y. Li, Z. F. Liu, *Langmuir* **2000**, *16*, 3846.
[25] A. Doron, E. Joselevich, A. Schlittner, A. Willner, *Thin Solid Films* **1999**, *340*, 183.
[26] T. Sato, D. G. Hasko, H. Ahmed, *J. Vac. Sci. Technol. B* **1997**, *15*, 45.
[27] K. J. Stevenson, G. J. Hurtt, J. T. Hupp, *Electrochem. Solid-State Lett.* **1999**, *2*, 175.
[28] Y. Xia, G. M. Whitesides, *Angew. Chem. Int. Ed.* **1998**, *37*, 550.
[29] O. O. Van der Biest, L. J. Vandeperre, *Annu. Rev. Mater. Sci.* **1999**, *29*, 327.
[30] C. P. Gutierrez, J. R. Mosley, T. C. Wallace, *J. Electrochem. Soc.* **1962**, *109*, 923.
[31] C. B. Ahlers, J. B. Talbot, *J. Electrochem. Soc.* **1999**, *146*, 3259.
[32] M. Holgado, F. Garcia-Santamaria, A. Blanco, M. Ibisate, A. Cintas, H. Miguez, C. J. Serna, C. Molpeceres, J. Requena, A. Mifsud, F. Meseguer, C. Lopez, *Langmuir* **1999**, *15*, 4701.
[33] T. Teranishi, M. Hosoe, T. Tanaka, M. Miyake, *J. Phys. Chem. B* **1999**, *103*, 3818.
[34] M. Trau, D. A. Saville, I. A. Aksay, *Science* **1996**, *272*, 706.
[35] M. Giersig, P. Mulvaney, *J. Phys. Chem.* **1993**, *97*, 6334.
[36] M. Giersig, P. Mulvaney, *Langmuir* **1993**, *9*, 3408.
[37] D. F. Evans, H. Wennerstrom, *The Colloidal Domain*, 2nd ed., Wiley-VCH, Weinheim **1999**. $F_N = v3\pi\eta d$, where v is the velocity of the colloid, η is the viscosity of the medium, and d is the diameter of the colloid (14 nm). The velocity at which the colloid moves in the absence of an electric field is described by the following equation [32]: $v = [d^2(\rho_s - \rho_w)g]/18\eta$, where ρ_s is the density of the colloid, ρ_w is the density of the medium, and g is the acceleration due to gravity. Using these relationships, v was calculated to be 1.7×10^{-8} m^2/s V and the net force on the colloid was estimated to equal 6.6×10^{-20} N. In the presence of an electric field, the force a colloid experiences is given by $F = Q_E E$ with Q_E, the surface charge, given by: $Q_E = u_E 3\pi\eta d$, where u_E is the electrophoretic mobility of the colloid and E is the applied voltage. The electrophoretic mobility can be estimated from the reported zeta potential, ζ = –35 mV [22], via the following relationship: $\zeta = 3/2\eta u_E/\varepsilon_r\varepsilon_0$, where ε_0 is the permittivity of free space and ε_r is the relative permittivity of the medium (assuming no significant deviation from that of water). These calculations gave a surface charge, $Q_E = -2.18 \times 10^{-18}$ C and a net force, $F = 5.5 \times 10^{-19}$ N.
[38] P. Sarkar, P. S. Nicholson, *J. Am. Ceram. Soc.* **1996**, *79*, 1987.
[39] M. Trau, D. A. Saville, I. A. Aksay, *Langmuir* **1997**, *13*, 6375.
[40] Y. Solomentsev, M. Bohmer, J. L. Anderson, *Langmuir* **1997**, *13*, 6058.
[41] Lateral particle measurements obtained from AFM images are larger by approximately a factor of four. If the particle is incompressible and spherical then the particle's height is a good approximation to the true particle size. See: W.-L. Shaiu, J. Vesenka, D. Jondle, E. Henderson, D. D. Larson, *J. Vac. Sci. Technol. A* **1993**, *11*, 820. Careful characterization of the tip radius allows deconvolution of the tip profile from the particle profile. See: K. A. Ramirez-Aguilar, K. F. Rowlen, *Langmuir* **1998**, *14*, 2562.
[42] Digital Instruments Nanoscope Command Reference Manual, Version 4.22ce **1997**.
[43] R. G. Freeman, K. C. Grabar, K. J. Allison, R. M. Bright, J. A. Davis, A. P. Guthrie, M. A. Hommer, M. A. Jackson, P. C. Smith, D. G. Walter, M. J. Natan, *Science* **1995**, *267*, 1629.
[44] T. R. Jensen, K. L. Kelly, A. A. Lazarides, G. C. Schatz, *J. Cluster Sci.* **1999**, *10*, 295.
[45] T. Okamoto, I. Yamaguchi, R. Kobayashi, *Opt. Lett.* **2000**, *25*, 372.
[46] A. C. Templeton, J. J. Pietron, R. W. Murray, P. Mulvaney, *J. Phys. Chem. B* **2000**, *104*, 564.
[47] K. A. Nelson, R. Casalegno, R. J. D. Miller, M. D. Fayer, *J. Chem. Phys.* **1982**, *77*, 1144.
[48] C. E. Jordan, R. M. Corn, *Anal. Chem.* **1997**, *69*, 1449.
[49] F. Nakajima, Y. Hirakawa, T. Kaneta, T. Imasaka, *Anal. Chem.* **1999**, *71*, 2262.
[50] J. H. Holtz, S. A. Asher, *Nature* **1997**, *389*, 829.
[51] P. Tournois, *Opt. Commun.* **1994**, *106*, 253.
[52] F. Sabary, J. C. Dudek, A. Septier, G. Granet, *Appl. Phys. Lett.* **1991**, *58*, 1991.
[53] J. A. Rogers, M. Meier, A. Dodabalapur, *Appl. Phys. Lett.* **1998**, *73*, 1766.
[54] A. Kumar, G. M. Whitesides, *Science* **1994**, *263*, 60.
[55] J. Turkevich, P. C. Stevenson, J. Hillier, *Discuss. Faraday Soc.* **1951**, *11*, 55.
[56] T. R. Jensen, M. L. Duval, K. L. Kelly, A. A. Lazarides, G. C. Schatz, R. P. Van Duyne, *J. Phys. Chem. B* **1999**, *103*, 9846.

Fast Magic-Angle Spinning and Double-Quantum ^{1}H Solid-State NMR Spectroscopy of Polyelectrolyte Multilayers**

By *Leonard N. J. Rodriguez*, *Susan M. De Paul*, *Christopher J. Barrett*, *Linda Reven*,* and *Hans W. Spiess**

The alternate adsorption of anionic and cationic polymers has become an increasingly important method for producing uniform thin polymer films.[1] Since a wide variety of charged molecules and polymers are amenable to this approach, polyelectrolyte multilayers (PEMs) are being explored for applications ranging from photonics to enzyme immobilization.

[*] Prof. L. Reven, L. N. J. Rodriguez, Prof. C. J. Barrett
Department of Chemistry, McGill University
801 Sherbrooke St. West
Montreal, Quebec, H3A 2K6 (Canada)
E-mail: lina_reven@maclan.mcgill.ca
Dr. S. M. De Paul, Prof. H. W. Spiess
Max-Planck-Institut für Polymerforschung
Postfach 3148, D-55021 Mainz (Germany)
E-mail: spiess@mpip-mainz.mpg.de

[**] The authors acknowledge financial support from the Natural Sciences and Engineering Council of Canada (NSERC).

  0935-9648/00/2412-1934 $ 17.50+.50/0